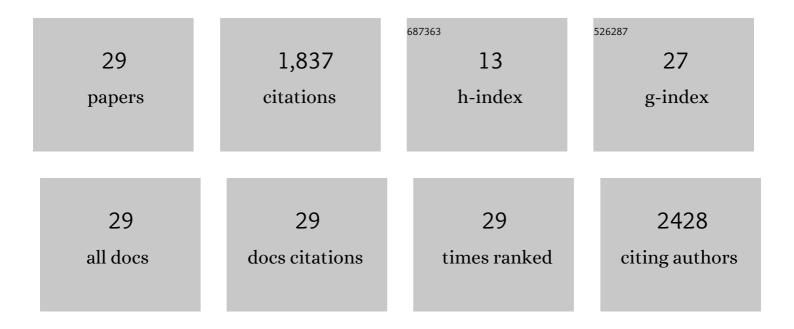
Hiromi Kimura-Suda

List of Publications by Year in descending order

Source: https://exaly.com/author-pdf/4471748/publications.pdf Version: 2024-02-01



#	Article	IF	CITATIONS
1	Base-Dependent Competitive Adsorption of Single-Stranded DNA on Gold. Journal of the American Chemical Society, 2003, 125, 9014-9015.	13.7	437
2	Quantitative Analysis and Characterization of DNA Immobilized on Gold. Journal of the American Chemical Society, 2003, 125, 5219-5226.	13.7	377
3	Independent control of grafting density and conformation of single-stranded DNA brushes. Proceedings of the National Academy of Sciences of the United States of America, 2007, 104, 9-14.	7.1	204
4	Quantitative Characterization of DNA Films by X-ray Photoelectron Spectroscopy. Langmuir, 2004, 20, 429-440.	3.5	185
5	Nucleobase Orientation and Ordering in Films of Single-Stranded DNA on Gold. Journal of the American Chemical Society, 2006, 128, 2-3.	13.7	153
6	Oligomerization and Pore Formation of a Sphingomyelin-specific Toxin, Lysenin. Journal of Biological Chemistry, 2003, 278, 22762-22770.	3.4	118
7	Alkanethiols on Platinum: Multicomponent Self-Assembled Monolayers. Langmuir, 2006, 22, 2578-2587.	3.5	113
8	Novel non-aggregated unsymmetrical metallophthalocyanines for second-order non-linear optics. Journal of Materials Chemistry, 1997, 7, 861-863.	6.7	59
9	Retention of fetuin-A in renal tubular lumen protects the kidney from nephrocalcinosis in rats. American Journal of Physiology - Renal Physiology, 2013, 304, F751-F760.	2.7	32
10	Magnesium prevents phosphate-induced vascular calcification via TRPM7 and Pit-1 in an aortic tissue culture model. Hypertension Research, 2017, 40, 562-567.	2.7	20
11	Vitamin K-dependent carboxylation of osteocalcin affects the efficacy of teriparatide (PTH1–34) for skeletal repair. Bone, 2014, 64, 95-101.	2.9	19
12	Mineral Composition of Phosphate-Induced Calcification in a Rat Aortic Tissue Culture Model. Journal of Atherosclerosis and Thrombosis, 2015, 22, 1197-1206.	2.0	17
13	Bone quality characteristics obtained by Fourier transform infrared and Raman spectroscopic imaging. Journal of Oral Biosciences, 2017, 59, 142-145.	2.2	15
14	Changes in Bone Quality Associated with the Mineralization of New Bone Formed Around Implants - Using XPS, Polarized Microscopy, and FTIR imaging Journal of Hard Tissue Biology, 2010, 19, 101-110.	0.4	11
15	Quantitative and Qualitative Analyses of Low-mineral-diet Ovariectomised Rat Femora Using Microscopic Computed Tomography. Journal of Hard Tissue Biology, 2011, 20, 107-114.	0.4	11
16	Studies on bone metabolism by using isotope microscopy, FTIR imaging, and micro-Raman spectroscopy. Journal of Oral Biosciences, 2013, 55, 61-65.	2.2	9
17	Collagen Fiber Orientation in the Femur of Rats with Chronic Kidney Disease. E-Journal of Surface Science and Nanotechnology, 2015, 13, 244-246.	0.4	9
18	Analysis of Collagen Fiber Orientation in Bone of Different Aged Rats Using FTIR Imaging. Molecular Crystals and Liquid Crystals, 2015, 622, 114-119.	0.9	8

#	Article	IF	CITATIONS
19	Simultaneous Determination of Average Direction of Molecular Orientation and Effective Second Order Nonlinear Optical Constant (d eff) by Phase Measurements of Second Harmonic Generation. Journal of Physical Chemistry B, 2001, 105, 1763-1769.	2.6	7
20	Quick and easy sample preparation without resin embedding for the bone quality assessment of fresh calcified bone using fourier transform infrared imaging. PLoS ONE, 2018, 13, e0189650.	2.5	7
21	Qualitative study of the New Bone formation Surrounding the Ti-implant by FTIR and Polarizing Microscope. Journal of Hard Tissue Biology, 2008, 17, 131-140.	0.4	7
22	Degree of orientations of collagen fibers and bone apatite crystals in rat femora by infrared dichroism imaging. Journal of Oral Biosciences, 2019, 61, 115-119.	2.2	6
23	Characterization and Controlled Properties of DNA Immobilized on Gold Surfaces. Kobunshi Ronbunshu, 2008, 65, 46-57.	0.2	3
24	Analysis of collagen fiber orientation in bone using infrared dichroism imaging in reflectance mode. Molecular Crystals and Liquid Crystals, 2017, 654, 244-248.	0.9	3
25	Comparison of the Efficacy and Renal Safety of Bisphosphonate Between Low-Dose/High-Frequency and High-Dose/Low-Frequency Regimens in a Late-Stage Chronic Kidney Disease Rat Model. Calcified Tissue International, 2020, 107, 389-402.	3.1	3
26	Relationships among collagen fiber orientation, mineralization, mineral maturity, and crystallinity. Molecular Crystals and Liquid Crystals, 2020, 707, 154-160.	0.9	3
27	Effects of risedronate, alendronate, and minodronate alone or in combination with eldecalcitol on bone mineral density, quality, and strength in ovariectomized rats. Bone Reports, 2021, 14, 101061.	0.4	1
28	Anisotropic SHG Behaviors of Tolan Derivatives in Monolayer Assemblies Prepared by Horizontal Lifting Method with Rotation of Substrate. Molecular Crystals and Liquid Crystals, 1999, 337, 81-84.	0.3	0
29	Mineralization and orientation of apatite in rat femur. The Proceedings of the JSME Conference on Frontiers in Bioengineering, 2016, 2016.27, C110.	0.0	0